Ionic interactions of Ba^{2+} blockades in the MthK K^+ channel

Rui Guo,[1] Weizhong Zeng,[2] Hengjun Cui,[1] Liping Chen,[2] and Sheng Ye[1]

[1]Life Sciences Institute and Innovation Center for Cell Biology, Zhejiang University, Hangzhou 310058, China
[2]Howard Hughes Medical Institute, Department of Physiology, University of Texas Southwestern Medical Center, Dallas, TX 75390

The movement and interaction of multiple ions passing through in single file underlie various fundamental K^+ channel properties, from the effective conduction of K^+ ions to channel blockade by Ba^{2+} ions. In this study, we used single-channel electrophysiology and x-ray crystallography to probe the interactions of Ba^{2+} with permeant ions within the ion conduction pathway of the MthK K^+ channel. We found that, as typical of K^+ channels, the MthK channel was blocked by Ba^{2+} at the internal side, and the Ba^{2+}-blocking effect was enhanced by external K^+. We also obtained crystal structures of the MthK K^+ channel pore in both Ba^{2+}–Na^+ and Ba^{2+}–K^+ environments. In the Ba^{2+}–Na^+ environment, we found that a single Ba^{2+} ion remained bound in the selectivity filter, preferably at site 2, whereas in the Ba^{2+}–K^+ environment, Ba^{2+} ions were predominantly distributed between sites 3 and 4. These ionic configurations are remarkably consistent with the functional studies and identify a molecular basis for Ba^{2+} blockade of K^+ channels.

The Journal of General Physiology

INTRODUCTION

K^+ channels catalyze selective and rapid transport of K^+ ions across the cell membrane (Hille, 2001). The combination of two apparently contradictory characteristics, strong selectivity for K^+ over other cations and very high K^+ conductance, arises from the presence of multiple ions moving and interacting in single file (Hodgkin and Keynes, 1955; Hille and Schwarz, 1978). The crystal structures of KcsA K^+ channel in its closed state (Fig. 1, left) reveal an ion conduction pathway that consists of a selectivity filter with four dehydrated K^+ ion–binding sites (S1–S4, extracellular to intracellular) formed by 20 oxygen atoms from backbone carbonyl and side-chain hydroxyl groups and an adjacent central cavity containing hydrated ions (Doyle et al., 1998; Zhou et al., 2001). Such an ion conduction pathway allows multiple K^+ ions to simultaneously occupy inside and to interact with each other, warranting the very high conductance and strong K^+ selectivity (Morais-Cabral et al., 2001).

Ba^{2+} is the only alkaline earth metal that blocks K^+ channels, presumably because it uniquely shares high similarity with the alkali metal K^+ in terms of the ionic radius (1.35 Å of Ba^{2+} vs. 1.33 Å of K^+) while doubling the charge. The similar size allows Ba^{2+} ions to fit into the K^+ channel selectivity filter. However, the charge apparently causes tight binding, preventing the rapid flow of K^+. The inhibitory properties of Ba^{2+} ions on K^+ channels have been extensively used to functionally probe the K^+ channel structure (Armstrong and Taylor, 1980; Vergara and Latorre, 1983; Neyton and Miller, 1988a,b; Piasta et al., 2011). Among these studies, Neyton and Miller (1988a,b) showed that Ba^{2+} inhibition of Ca^{2+}-activated K^+ channels is sensitive to the K^+ ions externally or internally, and they identified three K^+-binding sites with different affinities and effects on Ba^{2+} blockades. An external lock-in site preferentially binds K^+ ions with high affinity over Na^+ ions by a factor of ~1,000. K^+ binding at the external lock-in site prevents Ba^{2+} ions from exiting to the external side. Higher external concentration (500 mM) causes K^+ binding at an enhancement site, driving Ba^{2+} ions to dissociate rapidly to the internal side. Internal K^+ ions also cause a similar lock-in effect, whereas the internal lock-in site is nonselective for both K^+ and Na^+. These studies suggest that the ion conduction pathway of K^+ channels contains multiple distinct ion-binding sites. The determination of the first K^+ channel structure (Doyle et al., 1998) invoked structural interpretations of these phenomena (Jiang and MacKinnon, 2000). Ba^{2+}-soaked KcsA crystal structure in the absence of K^+ showed that Ba^{2+} ions preferably bind at sites 2 and 4 (Lockless et al., 2007). However, experimental and computational studies of Ba^{2+} blockades in the KcsA K^+ channels yielded different interpretations of Ba^{2+} blockades (Kim and Allen, 2011; Piasta et al., 2011; Rowley and Roux, 2013), so further studies are needed.

The structures of the isolated ion conduction pore of MthK in its open conductive state (Fig. 1, right) revealed a similar selectivity filter and a central cavity (Ye et al., 2010), whereas the high resolution allowed us to probe the Ba^{2+} block mechanism in a more highly accurate structural way than the earlier studies (Jiang and MacKinnon, 2000; Lockless et al., 2007). In this current

Correspondence to Sheng Ye: sye@zju.edu.cn

The Rockefeller University Press $30.00
J. Gen. Physiol. Vol. 144 No. 2 193–200
www.jgp.org/cgi/doi/10.1085/jgp.201411192

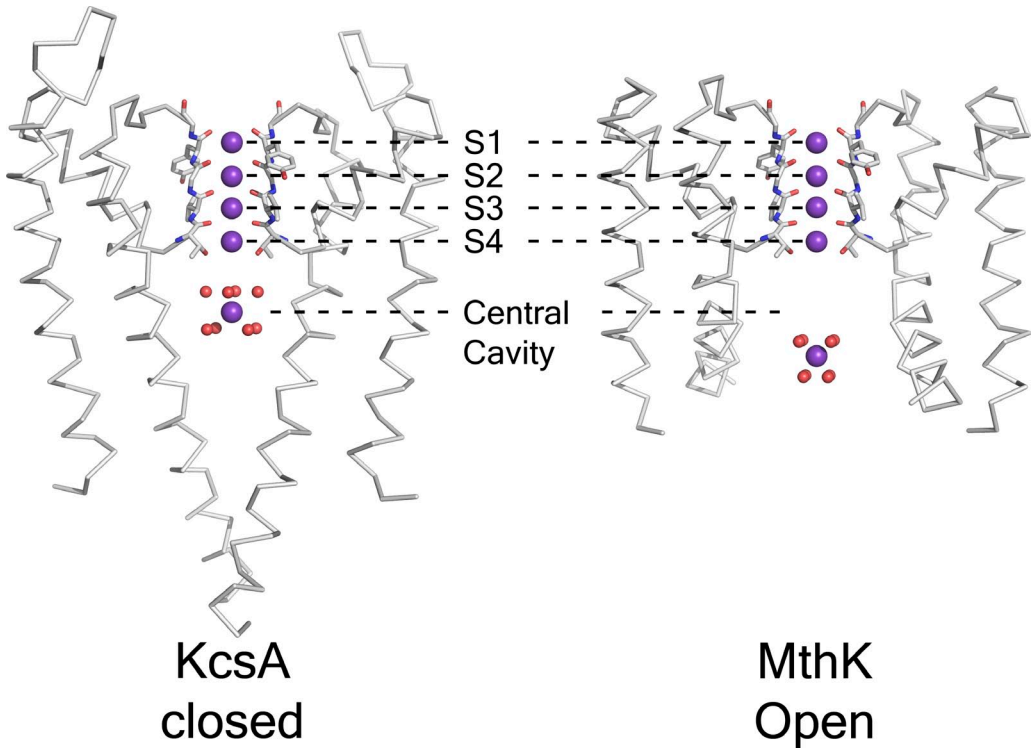

Figure 1. Structures of KcsA and MthK K^+ channels and the selectivity filters. Two opposing subunits (Cα trace) of KcsA and MthK K^+ channels with carbonyl oxygens (red sticks) are shown in the selectivity filter. The K^+-binding sites are indicated.

study, we characterized the Ba^{2+} blockades of MthK K^+ channel at the single-channel level and demonstrated that the MthK K^+ channel displays a typical K^+ channel Ba^{2+} blockade property. We further determined the positions of Ba^{2+} ions in the pore of MthK K^+ channel at two different ionic environments, which allowed us to deduce ionic configurations and to analyze the interactions of Ba^{2+} ions and the permeation ions.

MATERIALS AND METHODS

Electrophysiological study

The MthK K^+ channel was expressed and purified in *n*-decyl-β-D-maltoside as described previously (Jiang et al., 2002). Purified MthK A88D mutant was reconstituted into lipid vesicles composed of 3:1 POPE/POPG. To increase the fusion efficiency of the channel in the synthetic lipid bilayers, protein/lipid ratios of 1:100 were used in the reconstitution. Single-channel data were recorded in a vertical lipid bilayer setup in which a planar lipid bilayer of 3:1 POPE/POPG (20 mg/ml) in decane was painted over an ∼150-µm hole in a polystyrene partition separating the internal and external solutions. To induce fusion of channel-containing vesicles, the solution on the side to which vesicles were added (external side) contained 150 mM NaCl and 10 mM Tris, pH 8.0, whereas the opposite side (internal side) contained 15 mM KCl and 10 mM Tris, pH 8.0. After the appearance of channels in the membrane, as monitored under voltage pulses, KCl concentration in the internal solution was raised to 150 mM. Ba^{2+} was added only to the intracellular side of the channel. Membrane voltage was controlled and current was recorded using an amplifier (Axopatch 200B; Molecular Devices) with an analogue-to-digital converter (Digidata 1322A; Axon Instruments). Currents were low-pass filtered at 1–2 kHz and sampled at 10 kHz.

Crystallization, data collection, and structure determination

The MthK K^+ channel pores were purified and crystallized as described previously (Ye et al., 2010). The crystals were soaked either in a solution containing 3.5 M 1,6-hexandiol, 10 mM $BaCl_2$, 100 mM NaCl, 5 mM LDAO, and 100 mM HEPES, pH 7.5 (Ba^{2+}–Na^+ complex), or in an otherwise identical solution containing 10 mM $BaCl_2$ and 100 mM KCl (Ba^{2+}–K^+ complex) overnight. To avoid the interference of the Na^+ ion, if any, we neutralized the HEPES buffer with KOH for the Ba^{2+}/K^+ soaking solution. The soaked crystals were directly frozen in liquid nitrogen. X-ray data were collected at the Shanghai Synchrotron Radiation Facility BL17U beamline. The data were indexed, integrated, and scaled using the program HKL-2000 (HKL Research, Inc.; Otwinowski and Minor, 1997). The structures were determined by molecular replacement using Phaser in the CCP4 suite (Collaborative Computational Project, Number 4, 1994) with the MthK pore structure (Protein Data Bank accession no. 3LDC) as a search model, followed by model building with XtalView (McRee, 1999) and refinement with REFMAC (Collaborative Computational Project, Number 4, 1994). Detail data collection and refinement statistics are listed in Table 1. The structure coordinates and reflection files are deposited in the Protein Data Bank under accession nos. 4QE7 and 4QE9.

One-dimensional electron density profiles

We obtained one-dimensional electron density profiles of bound ions in the selectivity filter as described previously (Morais-Cabral et al., 2001). All data were scaled to 2.4-Å resolution against the K^+ complex crystal (100 mM K^+; Protein Data Bank accession no. 3LDC) before map calculation. We obtained one-dimensional profiles by sampling the Fo–Fc difference maps or the anomalous

TABLE 1

Data collection and refinement statistics

Statistics	Protein	
	Ba^{2+},K^+–MthK complex	Ba^{2+},Na^+–MthK complex
Mutations	S68H, V77C	S68H, V77C
$BaCl_2$/KCl/NaCl concentration	10 mM/100 mM/0 mM	10 mM/0 mM/100 mM
Data collection		
Space group	$P42_12$	$P42_12$
Unit cell a, c (Å)	61.0, 45.0	61.0, 45.3
Resolution (Å)	2.15	2.4
Measured reflections	51,128	42,306
Unique reflections	4,888	3,576
Redundancy	10.5	11.8
Completeness (%)	98.4 (100.0)	97.5 (91.3)
Mean I/σ	26.6 (2.4)	41.2 (2.1)
R_{sym} (%)	10.5 (75.3)	9.2 (72.1)
Refinement		
Resolution (Å)	50.0–2.15	50.0–2.4
R_{work}/R_{free} (%)	19.8/25.7	22.1/26.5
Number of protein atoms	648	633
Number of K^+ ions	6	0
Number of Na^+ ions	0	0
Number of Ba^{2+} ions	0	3
Number of water molecules	43	28
RMSD bond lengths (Å)	0.010	0.009
RMSD bond angles (°)	1.15	1.13

Numbers in parentheses are statistics for highest resolution shell. Redundancy = total measurements/unique reflections. $R_{sym} = \Sigma|Ii - <Ii>|/\Sigma Ii$, where <Ii> is the mean intensity of symmetry equivalent reflections. $R_{work} = \Sigma|F(obs) - F(cal)|/\Sigma F(obs)$. 10% of the data was used in the R_{free} calculations. RMSD, root mean square deviation.

difference maps, with ions and selectivity filter residues omitted, along the central axis of the filter using MAPMAN (Kleywegt and Jones, 1996). Occupancies were estimated for Ba^{2+}–Na^+ and Ba^{2+}–K^+ complexes by comparing one-dimensional electron density profiles with that of the K^+ complex as a standard of known occupancy based on the assumption that the relative peak areas in one-dimensional electron density maps calculated from these model maps were nearly proportional to the relative number of electrons in the model ion.

RESULTS

Ba^{2+} blockades in the MthK K^+ channel

A purified MthK A88D mutant channel was reconstituted into lipid vesicles, and its functional properties were studied in a vertical lipid bilayer membrane. We chose A88D mutant instead of wild-type MthK channel in this study because this mutant channel is constitutively active with extremely high open probability in the absence of Ca^{2+} (Shi et al., 2011), which allows us to record the single-channel outward current by avoiding the reduction of the outward conductance caused by intracellular [Ca^{2+}] (Zadek and Nimigean, 2006; Li et al., 2007).

Fig. 2 A shows sample traces of the outward currents of this mutant recorded at 100 mV with 150 mM K^+ at internal and 150 mM Na^+ at external sides. The channel is fully open, with only rapid closings within a burst (intraburst closings). The dwell time distributions of the closed states can be fit with one exponential component, as shown beside the trace (Fig. 2 A). The time constant of the rapid intraburst closings ($\tau_{intraburst}$) is 0.76 ms, similar to that of a wild-type channel from an earlier study, indicating that it is an intrinsic property of the ion conduction pore (Li et al., 2007).

200 µM Ba^{2+} was then added to the internal side of the channel to induce block (Fig. 2 B), whereas ∼10 mM Ba^{2+} was needed to see significant blockade effect at the external side (Fig. 2 D), indicating that the MthK channel shares an asymmetric Ba^{2+} blockade with many other K^+ channels (Standen and Stanfield, 1978a,b; Armstrong and Taylor, 1980; Armstrong et al., 1982; Vergara and Latorre, 1983; Piasta et al., 2011). As shown in Fig. 2 B, the addition of an internal 200 µM Ba^{2+} induces interburst in addition to the intraburst closings. Analysis of the dwell time distributions of the closed states gives rise to a $\tau_{intraburst}$ of 0.83 ms and a time constant for the interburst closings ($\tau_{interburst}$) of 10.7 ms. The similar $\tau_{intraburst}$ before and after Ba^{2+} block indicates that this fast gating process is independent of added Ba^{2+} ions, whereas the interburst closings reflect channel-blocking events induced by Ba^{2+} ions. Similarly, the dwell time distribution of the closed states can be fit with two exponential components with 10 mM Ba^{2+} in the external side (Fig. 2 D).

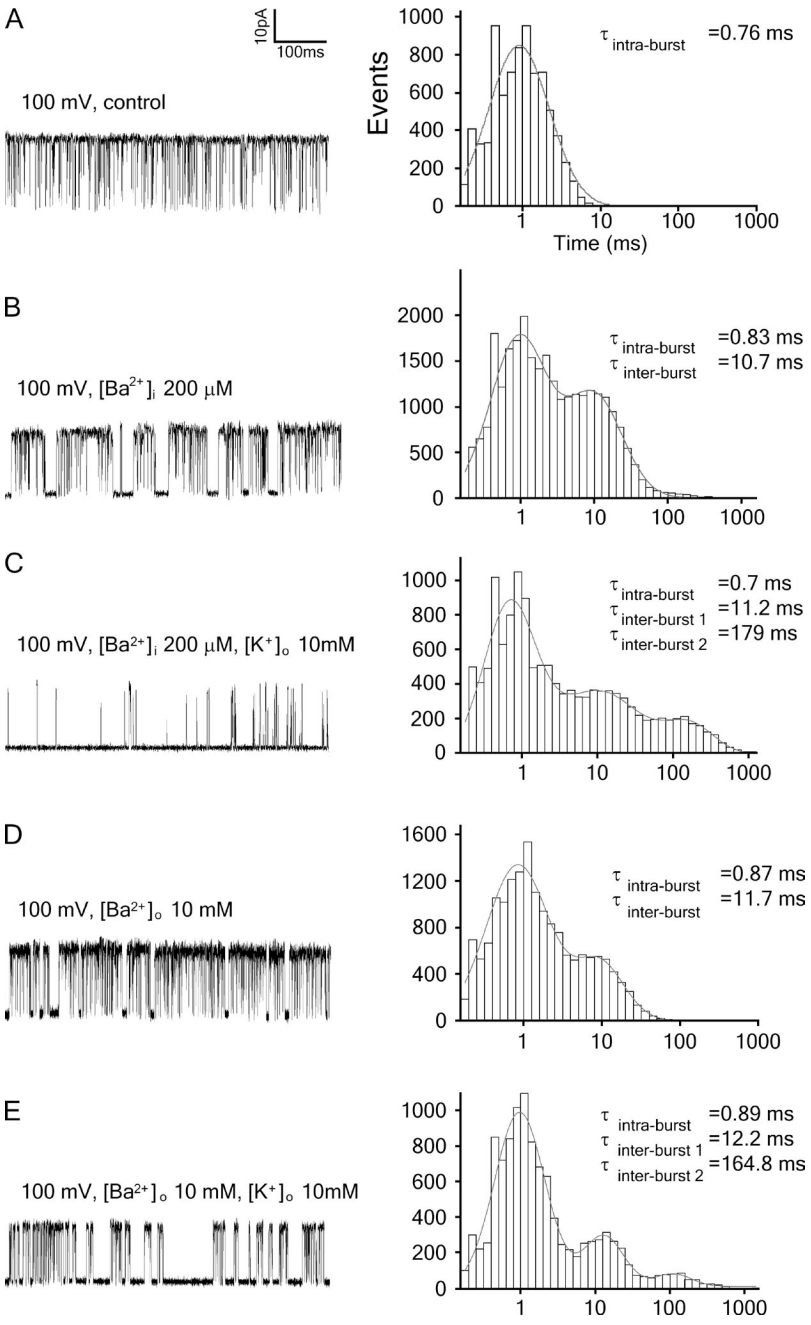

Figure 2. Ba^{2+} blockades of the MthK K^+ channel and kinetics analysis. A single MthK K^+ channel was observed in planar bilayers in the presence of 150 mM of internal KCl and 150 mM of external NaCl, with additional KCl added to the external medium. Blocks were induced with internal Ba^{2+}, and the holding potential was 100 mV. The dwell time distributions of the closed states are shown beside the traces. (A–E) Single-channel traces of MthK A88D mutant recorded at 100 mV (A); with 200 μM $BaCl_2$ added in the internal solution (B); with 200 μM $BaCl_2$ added in the internal and 10 mM KCl added in the external solutions (C); with 10 mM $BaCl_2$ added in the external solution (D); and with 10 mM $BaCl_2$ and 10 mM KCl added in the external solution (E).

The Ba^{2+} block kinetics is strongly affected by externally applied K^+ ions. As shown in Fig. 2 (C and E), 10 mM K^+ dramatically increased Ba^{2+} block duration. The dwell time distributions are fit by three well-separated exponentials of time constants of 0.7 ms ($\tau_{intraburst}$), 11.2 ms ($\tau_{interburst1}$), and 179 ms ($\tau_{interburst2}$) for internal Ba^{2+} blockade (Fig. 2 C) or of 0.89 ms ($\tau_{intraburst}$), 12.2 ms ($\tau_{interburst1}$), and 164.8 ms ($\tau_{interburst2}$) for external Ba^{2+} blockade (Fig. 2 E). This is very similar to the K^+ lock-in effect reported earlier on the BK channel (Neyton and Miller, 1988b) and recently on KcsA (Piasta et al., 2011). In addition to the intraburst closings, the interburst closings contain a shorter and longer duration fraction. The shorter one has a similar time constant ($\tau_{interburst1}$) to that without external K^+ ions (Fig. 2, B and D), whereas the external K^+ produces a much slower block component.

Ion occupancy in the selectivity filter

We soaked the MthK pore crystals in a stabilization solution containing 10 mM Ba^{2+} and 100 mM Na^+ (Ba^{2+}–Na^+ complex) or 10 mM Ba^{2+} and 100 mM K^+ (Ba^{2+}–K^+ complex) and determined their structures at 2.4- and 2.15-Å resolution, respectively (Table 1). To study the occupancy of Ba^{2+} ions in the selectivity filter at the Ba^{2+}–Na^+ environment, we first calculated the Fo–Fc electron density map of the Ba^{2+}–K^+ complex after omitting the

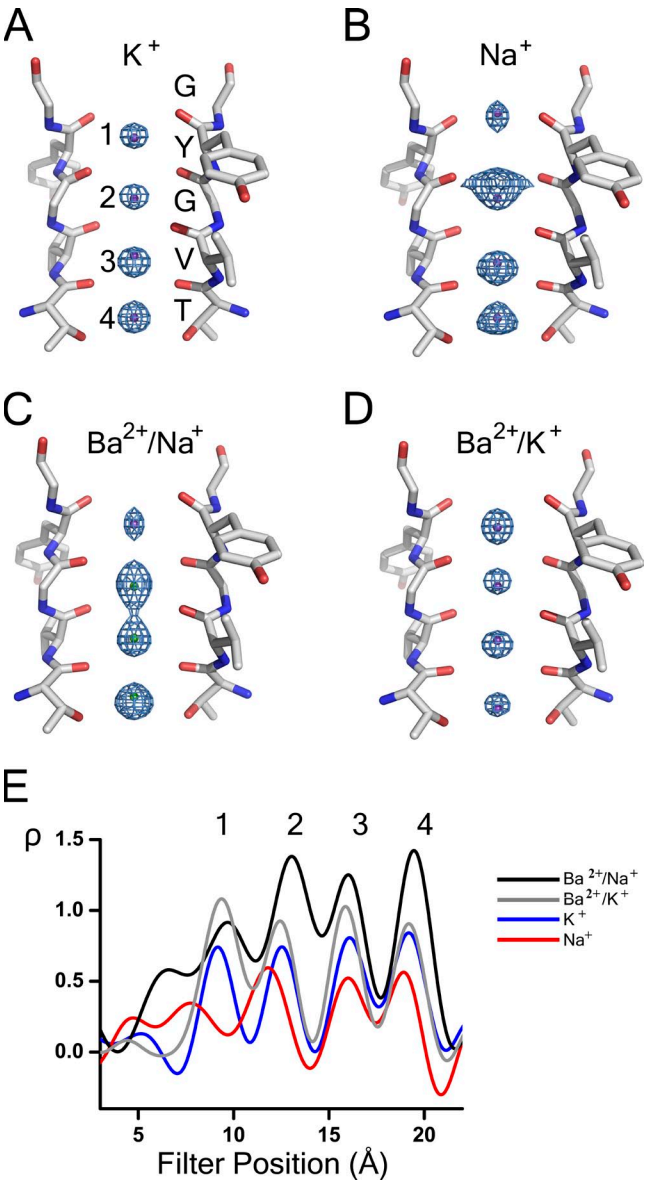

Figure 3. The selectivity filter of MthK in different environments. (A–D) Fo–Fc ion omit maps show the selectivity filter of two diagonally opposing subunits with bound ions. (A) Electron density map contoured at 5σ of the K^+ complex (in 100 mM K^+). The four K^+-binding sites in the filter are numbered 1 through 4. This result is based on an MthK structure that we have deposited into the Protein Data Bank (accession no. 3LDC). (B) Electron density map contoured at 2σ of the Na^+ complex (in 100 mM Na^+; Protein Data Bank accession no. 3LDE). (C) Electron density map contoured at 5σ of the Ba^{2+}–Na^+ complex (in 10 mM Ba^{2+} and 100 mM Na^+). (D) Electron density map contoured at 5σ of the Ba^{2+}–K^+ complex (in 10 mM Ba^{2+} and 100 mM K^+). (E) The one-dimensional electron density profiles along the central axis of the selectivity filter.

selectivity filter and ions (Fig. 3 C) and compared it with those at Na^+ and K^+ environments (Fig. 3, A and B). The electron density in the filter of the Ba^{2+}–Na^+ complex is stronger than that of the Na^+ complex (in 100 mM Na^+) and K^+ complex (in 100 mM K^+; Fig. 3 E), indicating

TABLE 2

The wavelength-dependent scattering factors (F′ and F″) of all the existing elements in the MthK crystals

Element	Wavelength	F′ (electron)	F″ (electron)
	Å		
Ba^{2+}	0.9786	−0.3116	3.9748
K^+	0.9786	0.2695	0.4627
S	0.9786	0.1824	0.2337
Na^+	0.9786	0.0568	0.0489
C	0.9786	0.0042	0.0033
N	0.9786	0.0088	0.0067
O	0.9786	0.0163	0.0122

that the selectivity filter is occupied by a heavier Ba^{2+} ion (56 electrons). By assuming that the area under the peaks of the one-dimensional electron density profile along the central axis of the filter reflects the number of electrons in the filter, we compared the one-dimensional electron density profiles and estimated an increase of 46 e^- compared with the Na^+ complex. This is roughly equivalent to the replacement of a Na^+ ion with a Ba^{2+} ion, suggesting that a single Ba^{2+} ion bound in the filter of the Ba^{2+}–Na^+ complex. Piasta et al. (2011) also determined that a single Ba^{2+} ion binds in and blocks the channel based on their blockade experiments, consistent with our estimation from the crystal structure. At the wavelength used for data collection (0.9786 Å), anomalous scattering of Ba^{2+} dominated in the protein (Table 2). We then calculated an anomalous difference Fourier map of the Ba^{2+}–Na^+ complex and observed nonequivalent Ba^{2+} occupancy at the four sites of the MthK filter (Fig. 4 A). The anomalous signal at site 2 is much stronger than that at sites 3 and 4, with no substantial signal observed at site 1. This suggests that the Ba^{2+} ion predominately occupies site 2 at the Ba^{2+}–Na^+ environment and has no binding at site 1.

The same analysis of the Ba^{2+}–K^+ complex revealed that the electron density in the filter of the Ba^{2+}–K^+ complex is substantially stronger than that of the K^+ complex (in 100 mM K^+; Fig. 3, D and E) but weaker than that of the Ba^{2+}–Na^+ complex (Fig. 3, C–E), indicating a partial Ba^{2+} ion bound in the filter of the Ba^{2+}–K^+ complex. The anomalous difference Fourier map of the Ba^{2+}–K^+ complex further revealed nonequivalent Ba^{2+} occupancy at the four sites of the MthK filter. However, different to that in the Ba^{2+}–Na^+ environment, Ba^{2+} ions predominately occupy sites 3 and 4 in the Ba^{2+}–K^+ environment and have no binding at sites 1 and 2 (Fig. 4, B and C).

DISCUSSION

In this study, we characterized the Ba^{2+} blockade property of the MthK K^+ channel at the single-channel level and further determined the positions of Ba^{2+} ions in the pore of the MthK K^+ channel at two different ionic environments (Ba^{2+}–Na^+ and Ba^{2+}–K^+). We concluded that

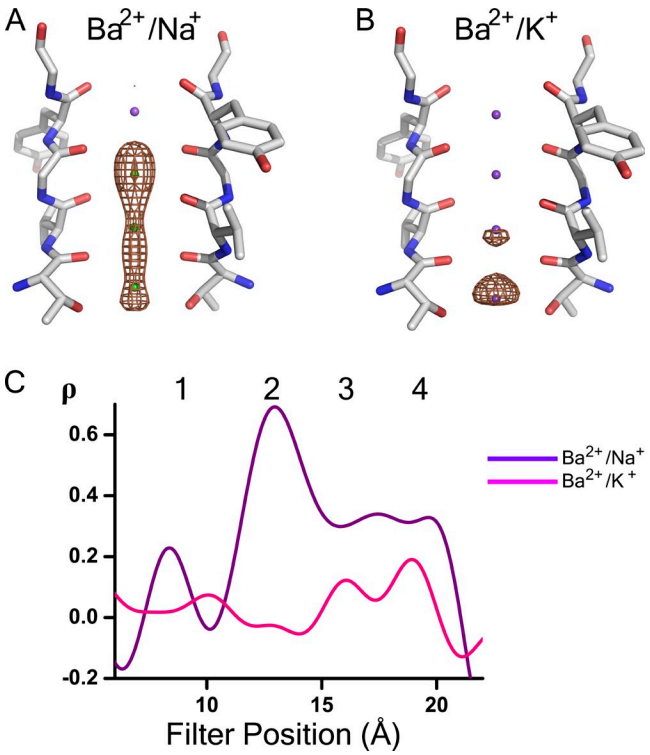

Figure 4. Ba^{2+} binding in the selectivity filter of MthK in Ba^{2+}–Na^+ and Ba^{2+}–K^+ environments. (A and B) Anomalous difference Fourier maps show the selectivity filter of two diagonally opposing subunits with bound ions. (A) Electron density map contoured at 4σ of the Ba^{2+}–Na^+ complex (in 10 mM Ba^{2+} and 100 mM Na^+). (B) Electron density map contoured at 3σ of the Ba^{2+}–K^+ complex (in 10 mM Ba^{2+} and 100 mM K^+). (C) The one-dimensional anomalous difference electron density profiles along the central axis of the selectivity filter.

the MthK K^+ channel shares a similar Ba^{2+} blockade property with other K^+ channels. Our main experimental observation is that, in the Ba^{2+}–Na^+ environment, a single Ba^{2+} ion shares occupancy among sites 2–4, predominately at site 2, and has no binding at site 1, whereas in the Ba^{2+}–K^+ environment, partial Ba^{2+} ion occupies sites 3 and 4 and has no binding at sites 1 and 2. This allows us to analyze the interactions of Ba^{2+} ions and the permeation ions and to provide structural interpretations of Ba^{2+} blockade of K^+ channels relating to the physical origins of K^+ channel selectivity.

Site 1 as a high energy barrier for Ba^{2+} ions

Our structural data are highly consistent with functional data of Ba^{2+} blockade on K^+ channels. The electrophysiological recordings showed that externally added Ba^{2+} also blocks the MthK K^+ channel, but at a concentration on the order of 10 mM, ∼50-fold higher than that required for internal block. Moreover, the external K^+ lock-in properties of external Ba^{2+} blocked states are identical to those induced by internal Ba^{2+}, indicating that Ba^{2+} enters the K^+ channel selectivity filter to induce block, but the energy barrier for entering the site is higher from the external solution than from the internal solution. This observation agrees well with the functional data on Ca^{2+}-activated K^+ channel showing that a concentration of 10 mM is required for external Ba^{2+} block, whereas a concentration of only 100 nM, ∼10,000-fold lower than that required for external block, is required for internal Ba^{2+} block (Vergara and Latorre, 1983). Similar asymmetric Ba^{2+} block was also observed in the delayed rectifier K^+ channel of squid (Armstrong and Taylor, 1980; Armstrong et al., 1982), the inward rectifier of muscle (Standen and Stanfield, 1978a,b), and KcsA (Piasta et al., 2011). Consistently, the ionic configurations deduced by x-ray crystallographic analysis on two ionic environments (Ba^{2+}–K^+ and Ba^{2+}–Na^+) revealed that Ba^{2+} rarely binds at site 1 of the MthK K^+ channel selectivity filter, indicative of a very low affinity of Ba^{2+} binding at site 1 close to the channel's outer mouth, and revealed a high energy barrier that limits Ba^{2+} to enter from, or exit to, the external side. Such a barrier does not seem to exist in the inner mouth of the channel, as the ionic configurations revealed Ba^{2+} bindings at sites 2–4. Interestingly, Ba^{2+} binding at site 1 was observed in NaK2K (see Lam et al. in this issue); correspondingly, external Ba^{2+} block in NaK2K is stronger than that in MthK (unpublished data).

A single Ba^{2+} ion binds in the K^+ channel selectivity filter

The estimation of a single Ba^{2+} ion bound in the filter of the Ba^{2+}–Na^+ complex raised an interesting question related to the Ba^{2+}-blocking mechanism of the K^+ channel. Why does only a single Ba^{2+} ion bind in the filter, instead of two, like that of alkali metal ions K^+, Rb^+, or Cs^+? Charge balance provides an explanation. The selectivity filter contains 20 oxygen atoms surrounding a 12-Å-long narrow pore. Each oxygen atom is associated with a partially negative charge. A charge balance exists between 20 partially negative oxygen atoms and two monovalent K^+ ions or one divalent Ba^{2+} ion. In addition, K^+ ions have been shown to simultaneously occupy 1,3 or 2,4 positions in the filter, but this binding configuration would seem to be unstable, as the repulsive force between two Ba^{2+} ions is fourfold that of K^+ ions. Therefore, Ba^{2+} ions cannot simultaneously occupy 1,3 or 2,4 positions in the filter, with 1,4 positions becoming possible. The very low affinity of Ba^{2+} binding at site 1 would then result in such a single Ba^{2+} ion binding in the filter.

When a single divalent Ba^{2+} ion binds in the MthK filter, can a monovalent Na^+ reside in the filter? It is difficult to distinguish Na^+ ions from water molecules based on the electron density map, as both have an equal number of electrons. However, the Na^+ binding at site 1 of the MthK filter adopts a pyramidal Na^+ coordination (Ye et al., 2010). This unique coordination has not been observed in the Ba^{2+}–Na^+ complex structure, indicating that Ba^{2+} binding predominately at site 2 drives most of the Na^+ ions out of site 1. Because the repulsive force

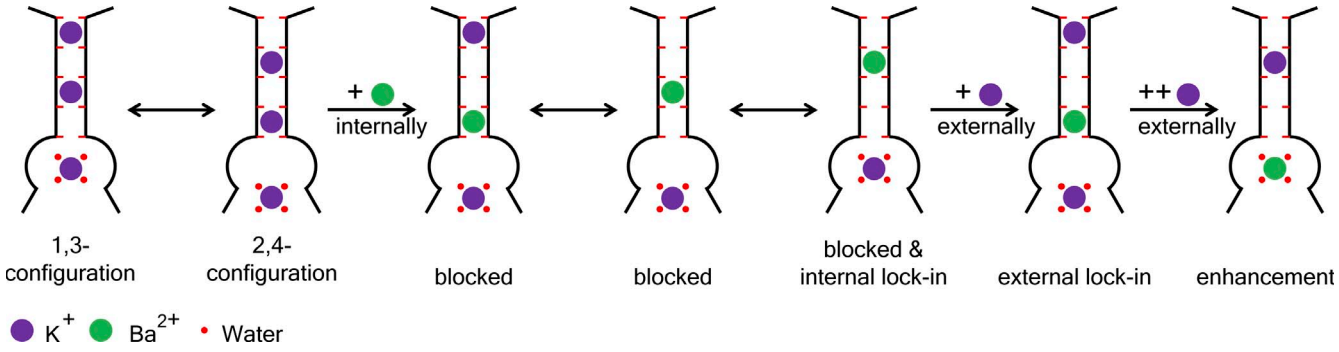

Figure 5. A mechanistic model of Ba^{2+} blockade at the selectivity filter.

between a Ba^{2+} ion and a Na^+ ion is twofold that of K^+ ions, Ba^{2+} and Na^+ ions simultaneously occupying 1,3 or 2,4 positions in the filter would seem to be an unstable binding configuration for electrostatic reasons. Therefore, with a single divalent Ba^{2+} ion bound in the MthK filter, only a partial Na^+ ion binds in the filter.

Interaction of Ba^{2+} and K^+ ions in the K^+ channel selectivity filter

A central feature of all K^+ channels is that their selectivity filters have a preference for K^+ ions over other cations. Among all four sites of the K^+ channel selectivity filter, site 1 is more highly selective for K^+ ions than other cations, especially Na^+ ions, as at a low K^+/high Na^+ condition, K^+ prefers sites 1 and 3 in MthK (Ye et al., 2010) and sites 1 and 2 in NaK2K (Sauer et al., 2013) K^+ channels. In the Ba^{2+}–K^+ environment, K^+ ions dominate the MthK filter, leaving a partial Ba^{2+} ion bound mainly at sites 3 and 4. This ionic configuration allows us to deduce a molecular basis for external lock-in and enhancement effects. At low K^+ concentration, a K^+ ion enters the MthK filter from external solution and binds preferably at site 1. The repulsive force between a K^+ ion and a Ba^{2+} ion is twice that of two K^+ ions, which drives the Ba^{2+} ion to move internally and mainly binds at site 4. However, at high K^+ concentration, K^+ ion further enters site 2, or even site 3. K^+ and Ba^{2+} ions simultaneously occupying 2,4 positions in the filter is a relatively unstable binding configuration, which explains why the effective K_d for achieving the external enhancement effect is nearly 500 mM (Neyton and Miller, 1988a). Such an unstable binding configuration forces Ba^{2+} dissociation to the internal side by the electrostatic repulsion. The ionic configuration in the Ba^{2+}–Na^+ environment also suggests a molecular basis for the internal enhancement effect. Monovalent cation, either Na^+ or K^+, resides at the central cavity, effectively driving the Ba^{2+} ion to predominately bind at site 2 through the electrostatic repulsion.

A few recent studies proposed different interpretations of the external K^+ lock-in effect. Piasta et al. (2011) suggested that the K^+ ion binds at site 1 and locks the Ba^{2+} ion preferably at site 2. However, K^+ and Ba^{2+} ions simultaneously binding to adjacent sites 1 and 2 will have strong electrostatic repulsion in between and are highly unstable. Computational studies suggested that the K^+ ion binds at site 0 and locks Ba^{2+} ion preferably at site 2 (Kim and Allen, 2011; Rowley and Roux, 2013). We think site 0 is unlikely to be the lock-in site based on three reasons. First, site 0 does not have the square antiprism configuration and is unlikely to be selective for K^+. Second, site 0 is a very weak ion-binding site. The electron density at site 0 is much weaker than that of sites 1–4 in KcsA filter (Zhou et al., 2001), whereas there is no density at site 0 in MthK (Ye et al., 2010), indicating weak K^+ binding at site 0. Third, the voltage dependence suggests that the external lock-in site resides ∼15% inside (Neyton and Miller, 1988a).

Conclusions

Our high resolution structural data allow us to clearly define the internal and external lock-in and enhancement effects (Neyton and Miller, 1988a,b). As shown in Fig. 5, without Ba^{2+}, two K^+ ions bind equivalently in the 1,3 and 2,4 configurations. The electrostatic repulsion between them destabilizes the ions and lowers the K^+ ion–binding affinity. This allows an additional K^+ ion to enter the filter and to expel a bound K^+ ion from the opposite end, warranting the efficient conduction of K^+. With the addition of Ba^{2+} from the internal side, Ba^{2+} enters the filter and initiates block by occupying the S4 site. The electrostatic repulsion between Ba^{2+} and K^+ allows the Ba^{2+} ion to effectively drive out K^+ ions from the filter, leaving a single Ba^{2+} ion alternating between S2, S3, and S4 sites and blocking the passage of K^+ ions. Ba^{2+} ions may leave the filter either by dissociation back to the internal side or proceeding to the external side by overcoming the high energy barrier at site 1. The addition of external K^+ in low concentration causes K^+ ion binding at its high affinity site 1, locking Ba^{2+} at site 4 and preventing Ba^{2+} from exiting to the external side. Although external K^+ in high concentration allows the K^+ ion to enter site 2, it forces Ba^{2+} ion dissociation to the internal side by the electrostatic repulsion. The internal K^+, or other permeant ions, can occupy the central cavity,

locking the Ba^{2+} ion mainly at site 2 and preventing the Ba^{2+} ion from exiting to the internal side.

We thank Youxing Jiang for discussions and critical reviews of the manuscript and S. Huang and J. He at the Shanghai Synchrotron Radiation Facility for on-site assistance.

This work was supported in part by funds from the National Natural Science Foundation of China (grant 31370721), the Ministry of Science and Technology (grants 2014CB910300 and 2011CB910500), the Natural Science Foundation of Zhejiang Province (grant R2100439), the Specialized Research Fund for the Doctoral Program of Higher Education (grant 20110101110122), and the Fundamental Research Funds for the Central Universities (grant to S. Ye).

The authors declare no competing financial interests.

Kenton J. Swartz served as editor.

Submitted: 1 March 2014
Accepted: 25 June 2014

REFERENCES

Armstrong, C.M., and S.R. Taylor. 1980. Interaction of barium ions with potassium channels in squid giant axons. *Biophys. J.* 30:473–488. http://dx.doi.org/10.1016/S0006-3495(80)85108-3

Armstrong, C.M., R.P. Swenson Jr., and S.R. Taylor. 1982. Block of squid axon K channels by internally and externally applied barium ions. *J. Gen. Physiol.* 80:663–682. http://dx.doi.org/10.1085/jgp.80.5.663

Collaborative Computational Project, Number 4. 1994. The CCP4 suite: programs for protein crystallography. *Acta Crystallogr. D Biol. Crystallogr.* 50:760–763. http://dx.doi.org/10.1107/S0907444994003112

Doyle, D.A., J. Morais Cabral, R.A. Pfuetzner, A. Kuo, J.M. Gulbis, S.L. Cohen, B.T. Chait, and R. MacKinnon. 1998. The structure of the potassium channel: Molecular basis of K^+ conduction and selectivity. *Science.* 280:69–77. http://dx.doi.org/10.1126/science.280.5360.69

Hille, B. 2001. Ionic Channels of Excitable Membranes. Third edition. Sinauer Associates, Sunderland, MA. 814 pp.

Hille, B., and W. Schwarz. 1978. Potassium channels as multi-ion single-file pores. *J. Gen. Physiol.* 72:409–442. http://dx.doi.org/10.1085/jgp.72.4.409

Hodgkin, A.L., and R.D. Keynes. 1955. The potassium permeability of a giant nerve fibre. *J. Physiol.* 128:61–88.

Jiang, Y., and R. MacKinnon. 2000. The barium site in a potassium channel by x-ray crystallography. *J. Gen. Physiol.* 115:269–272. http://dx.doi.org/10.1085/jgp.115.3.269

Jiang, Y., A. Lee, J. Chen, M. Cadene, B.T. Chait, and R. MacKinnon. 2002. Crystal structure and mechanism of a calcium-gated potassium channel. *Nature.* 417:515–522. http://dx.doi.org/10.1038/417515a

Kim, I., and T.W. Allen. 2011. On the selective ion binding hypothesis for potassium channels. *Proc. Natl. Acad. Sci. USA.* 108:17963–17968. http://dx.doi.org/10.1073/pnas.1110735108

Kleywegt, G.J., and T.A. Jones. 1996. *xdlMAPMAN* and *xdlDATAMAN*-programs for reformatting, analysis and manipulation of biomacromolecular electron-density maps and reflection data sets. *Acta Crystallogr. D Biol. Crystallogr.* 52:826–828. http://dx.doi.org/10.1107/S0907444995014983

Lam, Y., W. Zeng, D.B. Sauer, and Y. Jiang. 2014. The conserved potassium channel filter can have distinct ion binding profiles: Structural analysis of rubidium, cesium, and barium binding in NaK2K. *J. Gen. Physiol.* 144:181–192.

Li, Y., I. Berke, L. Chen, and Y. Jiang. 2007. Gating and inward rectifying properties of the MthK K^+ channel with and without the gating ring. *J. Gen. Physiol.* 129:109–120. http://dx.doi.org/10.1085/jgp.200609655

Lockless, S.W., M. Zhou, and R. MacKinnon. 2007. Structural and thermodynamic properties of selective ion binding in a K^+ channel. *PLoS Biol.* 5:e121. http://dx.doi.org/10.1371/journal.pbio.0050121

McRee, D.E. 1999. XtalView/Xfit—a versatile program for manipulating atomic coordinates and electron density. *J. Struct. Biol.* 125:156–165. http://dx.doi.org/10.1006/jsbi.1999.4094

Morais-Cabral, J.H., Y. Zhou, and R. MacKinnon. 2001. Energetic optimization of ion conduction rate by the K^+ selectivity filter. *Nature.* 414:37–42. http://dx.doi.org/10.1038/35102000

Neyton, J., and C. Miller. 1988a. Discrete Ba2+ block as a probe of ion occupancy and pore structure in the high-conductance Ca2+-activated K+ channel. *J. Gen. Physiol.* 92:569–586. http://dx.doi.org/10.1085/jgp.92.5.569

Neyton, J., and C. Miller. 1988b. Potassium blocks barium permeation through a calcium-activated potassium channel. *J. Gen. Physiol.* 92:549–567. http://dx.doi.org/10.1085/jgp.92.5.549

Otwinowski, Z., and W. Minor. 1997. Processing of X-ray diffraction data collected in oscillation mode. *Methods Enzymol.* 276:307–326. http://dx.doi.org/10.1016/S0076-6879(97)76066-X

Piasta, K.N., D.L. Theobald, and C. Miller. 2011. Potassium-selective block of barium permeation through single KcsA channels. *J. Gen. Physiol.* 138:421–436. http://dx.doi.org/10.1085/jgp.201110684

Rowley, C.N., and B. Roux. 2013. A computational study of barium blockades in the KcsA potassium channel based on multi-ion potential of mean force calculations and free energy perturbation. *J. Gen. Physiol.* 142:451–463. http://dx.doi.org/10.1085/jgp.201311049

Sauer, D.B., W. Zeng, J. Canty, Y. Lam, and Y. Jiang. 2013. Sodium and potassium competition in potassium-selective and non-selective channels. *Nat. Commun.* 4:2721. http://dx.doi.org/10.1038/ncomms3721

Shi, N., W. Zeng, S. Ye, Y. Li, and Y. Jiang. 2011. Crucial points within the pore as determinants of K^+ channel conductance and gating. *J. Mol. Biol.* 411:27–35. http://dx.doi.org/10.1016/j.jmb.2011.04.058

Standen, N.B., and P.R. Stanfield. 1978a. A potential- and time-dependent blockade of inward rectification in frog skeletal muscle fibres by barium and strontium ions. *J. Physiol.* 280:169–191.

Standen, N.B., and P.R. Stanfield. 1978b. Potential-dependent blockade by $Ba2^+$ of resting potassium permeability of frog sartorius [proceedings]. *J. Physiol.* 277:70P–71P.

Vergara, C., and R. Latorre. 1983. Kinetics of Ca2+-activated K+ channels from rabbit muscle incorporated into planar bilayers. Evidence for a Ca2+ and Ba2+ blockade. *J. Gen. Physiol.* 82:543–568. http://dx.doi.org/10.1085/jgp.82.4.543

Ye, S., Y. Li, and Y. Jiang. 2010. Novel insights into K^+ selectivity from high-resolution structures of an open K^+ channel pore. *Nat. Struct. Mol. Biol.* 17:1019–1023. http://dx.doi.org/10.1038/nsmb.1865

Zadek, B., and C.M. Nimigean. 2006. Calcium-dependent gating of MthK, a prokaryotic potassium channel. *J. Gen. Physiol.* 127:673–685. http://dx.doi.org/10.1085/jgp.200609534

Zhou, Y., J.H. Morais-Cabral, A. Kaufman, and R. MacKinnon. 2001. Chemistry of ion coordination and hydration revealed by a K^+ channel-Fab complex at 2.0 Å resolution. *Nature.* 414:43–48. http://dx.doi.org/10.1038/35102009